Tree Physiology 39, 628–640
doi:10.1093/treephys/tpy126

Research paper

Characterization and comparison of nitrate fluxes in *Tamarix ramosissima* and cotton roots under simulated drought conditions

Lin Zhang[1,2,†], Guangjie Li[1,†], Gangqiang Dong[3], Meng Wang[1], Dongwei Di[1], Herbert J. Kronzucker[4] and Weiming Shi[1,5]

[1]State Key Laboratory of Soil and Sustainable Agriculture, Institute of Soil Science, Chinese Academy of Sciences, No. 71 East Beijing Road, Nanjing 210008, China; [2]University of the Chinese Academy of Sciences, No.19(A) Yuquan Road, Shijingshan District, Beijing 100049, China; [3]Amway (China) Botanical R&D Center, Wuxi, Jiangsu 214115, China; [4]School of Agriculture and Food, Faculty of Veterinary and Agricultural Sciences, The University of Melbourne, Parkville, VIC 3010, Australia; [5]Corresponding author (wmshi@issas.ac.cn)

Received May 10, 2018; accepted November 23, 2018; published online December 19, 2018; handling Editor Torgny Näsholm

Tamarix ramosissima Ledeb., a major host plant for the parasitic angiosperm *Cistanche tubulosa*, and known for its unique drought tolerance, has significant ecological and economic benefits. However, the mechanisms of nitrogen acquisition by the *T. ramosissima* root system under drought have remained uncharacterized. Here, uptake of nitrate (NO_3^-) in various regions of the root system was measured in *T. ramosissima* using Non-invasive Micro-test Technology at the cellular level, and using a $^{15}NO_3^-$-enrichment technique at the whole-root level. These results were compared with responses in the model system cotton (*Gossypium hirsutum* L.). *Tamarix ramosissima* had lower net NO_3^- influx and a significantly lower K_m (the apparent Michalis–Menten constant; 8.5 μM) for NO_3^- uptake than cotton under normal conditions. Upon simulated drought conditions, using polyethylene glycol (PEG), NO_3^- flux in cotton switched from net influx to net efflux, with a substantive peak in the white zone (WZ) of the root. There were no significant NO_3^- influx signals observed in the WZ of *T. ramosissima* under control conditions, whereas PEG treatment significantly enhanced NO_3^- influx in the WZ of *T. ramosissima*. The effect of PEG application on NO_3^- fluxes was highly localized, and the increase in net NO_3^- influx in response to PEG stimulation was also found in *C. tubulosa*-inoculated *T. ramosissima*. Consistently, root nitrogen (N) content and root biomass were higher in *T. ramosissima* than in cotton under PEG treatment. Our study provides insights into NO_3^- uptake and the influence of *C. tubulosa* inoculation in *T. ramosissima* roots during acclimation to PEG-induced drought stress and provides guidelines for silvicultural practice and for breeding of *T. ramosissima* under coupled conditions of soil drought and N deficiency.

Keywords: *Cistanche tubulosa*, cotton, drought stress, nitrate uptake, NMT, *T. ramosissima*.

Introduction

The availability of nitrogen (N) is often a major factor limiting tree productivity as soil-N can be highly labile and subject to losses through leaching or by conversion to gaseous forms of N through denitrification, ammonification and ammonia oxidation (Coskun et al. 2017, Babst and Coleman 2018). In well-aerated forest soils, especially those in early successional and ruderal forest environments of the temperate zone, nitrification is rapid, and nitrate NO_3^- tends to be the primary N source available to plants (Kronzucker et al. 1997, Crawford and Forde 2002). Increasing evidence suggests that various plant species can take up organic N directly in the form of intact amino acids from soils (Näsholm et al. 2009, Warren 2014). More recently, several studies have been conducted in temperate (Warren 2009, Liu et al. 2017), subtropical (Li et al. 2015) and tropical (Liu et al. 2018) forests, showing that dominant tree species have the

---

[†]These authors contributed equally to this work.

capacity to take up organic N from soils. However, most species perform best on either NO_3^- or a mixed N source (Kronzucker et al. 1999). Plant species differ greatly in their capacities for the utilization of N and these adaptations may contribute to the unique spatial and/or temporal distributions of these species (Min et al. 2000, Kronzucker et al. 2003). For example, trembling aspen is a generalist species equally capable of thriving on low and high N; by contrast, kinetic parameters for N acquisition in lodgepole pine identify it as a specialist species particularly well adapted to high soil-N concentrations (Min et al. 2000).

Arid and semi-arid ecosystems are co-limited by the availability of both soil water and N (Zhang et al. 2013, Gessler et al. 2017), and N is frequently deficient in arid and semi-arid regions (Hernández et al. 1997). Drought-mediated reductions in environment N availability occur on account of decreased turnover rates for soil nutrients, decreased biomass input into soil and decreased movement of soil-N sources to the root surface (Liu et al. 2013). Plant responses to N fertilization under drought conditions vary with plant species, climate, N source and fertilization regime (Waraich et al. 2011). Many studies have found that NO_3^- is particularly important to drought resistance in arid environments (Houlton et al. 2007, Wang and Macko 2011). Nitrate has been reported to improve signaling in stomata closure (Wilkinson et al. 2007), and can also serve as an electron sink to alleviate photosystem stress under water-limitation conditions (Yi et al. 2014). Nitrate uptake is reduced under drought stress in many trees, such as poplar and beech (Rennenberg et al. 2006, Meng et al. 2016). Under drought conditions, higher N utilization can increase water-use efficiency and promote faster recovery after drought ceases (Gessler et al. 2017, Shi et al. 2017). However, despite a strong legacy of research on N dynamics in trees and in forest ecosystems and the rapidly growing literature on drought-induced mortality, there are few studies investigating the interaction between drought and N in trees (see review by Gessler et al. 2017) and the role of N in drought survival and mortality (Luo and Luo 2017, Shi et al. 2017). Moreover, we still know little about the physiological and biological mechanisms underpinning the optimization of N utilization to enhance drought tolerance in trees.

Tamarix ramosissima Ledeb., commonly known as saltcedar, plays important roles in desert ecosystems (Gries et al. 2005). It is native to Asia, where it is distributed widely, and is a notorious invasive species in North America (Stromberg et al. 2007, Walker 2008), Argentina, Australia and South Africa. As a halophyte with high resistance to drought, wind erosion and sand burial, *T. ramosissima* has been widely used in desertification control in China (Zhang and Zhang 2012). *Tamarix ramosissima* is widely considered strongly drought-tolerant (Cleverly et al. 1997). However, the physiological responses of *T. ramosissima* to drought stress are insufficiently understood, and few studies have reported how varying degrees of drought impacts such responses. In recent years, as the major host plant of the parasitic angiosperm *Cistanche tubulosa*, a profitable medicinal plant, the further economic benefits of *T. ramosissima* have begun to be discovered, such as in Xinjiang, China (Zhang and Zhang 2012). *Cistanche tubulosa* is a well-known edible and medicinal plant and has been referred to as the ‘ginseng of the desert’ (Jiang and Tu 2009). *Cistanche* is a perennial parasitic herb, relying on the host for its supply of solutes, both organic and inorganic, and water (Pignone and Hammer 2016). Thus, increasing the growth of the host plant *T. ramosissima* is a prerequisite to increasing the yield of *C. tubulosa*. A typical feature of soil fertility in desert regions is the lack of N, and drought and N deficiency are common in the arid Tarim Basin of Northwest China, where *T. ramosissima* is found, and total soil-N and organic matter contents are only $0.31\ g\ kg^{-1}$ and $2.42\ g\ kg^{-1}$, respectively (Min et al. 2018). Soil NO_3^- and ammonium contents have been measured at $10\ mg\ kg^{-1}$ and $1.5\ mg\ kg^{-1}$, respectively (unpublished data). In order to cope with its arid and N-impoverished growth environment, *T. ramosissima* has evolved a series of characteristics for N utilization. For example, *T. ramosissima* prefers to take up NO_3^- over ammonium, and NO_3^- increases the numbers of *T. ramosissima* roots and of infections of *C. tubulosa* (Luo et al. 2011). However, to the best of our knowledge, the mechanisms of NO_3^- uptake in zones of the *T. ramosissima* root system have not been explored and the roles of *C. tubulosa* inoculation and drought have not been investigated. Cotton (*Gossypium hirsutum* L.) is grown as a leading commercial crop in more than 30 countries (Riaz et al. 2013), and is also a dominant crop in Xinjiang, China. As a glycophyte, cotton shows higher tolerance to drought stress than other major crops (Hejnak et al. 2015) and has evolved several morpho-physiological strategies and molecular mechanisms against drought stress (Ullah et al. 2017). Given that the growth areas for *T. ramosissima* and cotton overlap in Xinjiang, China, cotton offers a good system for comparison with *T. ramosissima* when examining the responses of root N fluxes to drought.

In the present study, we conducted a greenhouse experiments to address the following questions: (i) What are the characteristics of NO_3^- uptake in zones of the *T. ramosissima* root system? (ii) How does drought impact NO_3^- uptake of *T. ramosissima*? (iii) How does *C. tubulosa* inoculation impact NO_3^- uptake of *T. ramosissima*? Here, *Gossypium hirsutum* cv. Xinhai 21, a widely cultivated variety of cotton in Xinjiang Province, China, was used as the model system for comparative analysis, and we measured N-kinetic parameters and steady-state as well as transient profiles of NO_3^- fluxes in different *T. ramosissima* root zones, using Non-invasive Micro-test Technology (NMT). We also investigated the effects of *C. tubulosa* inoculation and the imposition of drought on net NO_3^- fluxes, total N content and root growth in *T. ramosissima* and in cotton. Physiological mechanisms governing the interplay of root NO_3^- fluxes, plant response to *C. tubulosa* inoculation, and drought are discussed.

Materials and methods

Plant material and experimental design

A greenhouse experiment with a factorial design was conducted during 2015. *Tamarix ramosissima* cuttings (~18 cm in length, 1 cm in diameter) were obtained from 2-year-old stems collected from desert soil in the Hotan region, Xinjiang Province, and rooted in pots (~10 l) filled with fine sand. Columniform pots with a depth of 30 cm and a diameter of 25 cm were used in the experiment. Plants were cultivated in a greenhouse (natural light, day/night 28/23 °C, relative humidity: 60–75%) and irrigated every other day with 100 ml of Hoagland nutrient solution (Hoagland and Arnon 1950). After 50 days, when new roots and leaves had developed, similar saplings (~30 cm in height) were selected, and the root systems of the selected plants were carefully washed with tap water. Plants were then cultivated in hydroponics with modified Hoagland solution (KH_2PO_4, 0.2 mM; $MgSO_4$, 0.5 mM; $Ca(NO_3)_2$, 0.4 mM; $CaCl_2$ 1.0 mM; KCl, 1.5 mM; H_3BO_3, 1×10^{-3} mM; Na_2MoO_4, 5×10^{-5} mM; $CuSO_4$, 5×10^{-4} mM; $ZnSO_4$, 1×10^{-3} mM; $MnSO_4$, 1×10^{-3} mM; Fe(III)-EDTA, 0.1 mM, pH = 6.0). *Gossypium hirsutum* cv. Xinhai 21, a widely cultivated variety of cotton in Xinjiang Province, China, was used in the present study. Cotton seeds were placed on wet filter paper at 25 °C for ~24 h in the dark and then grown in sand that was irrigated every other day with Hoagland nutrient solution in a greenhouse identical to the *T. ramosissima* growth conditions. Cotton seedlings were transferred to modified nutrient solutions as above, once cotyledons were visible.

After pre-culturing for 2 weeks in aerated hydroponics with modified Hoagland's solution, the *T. ramosissima* and cotton seedlings were used for treatments. To test the effect of polyethylene glycol (PEG)-induced water stress on the root biomass and total N content, drought stress was applied for 1 week by adding 15% PEG 8000 (osmotic stress at 0.56 MPa, osmolarity of the solution was measured using a Wescor 5520 osmometer (VAPRO, Logan, UT, USA), and osmotic pressure was calculated as described in Money (1989)) to the nutrient solution described above, and seedlings grown in the nutrient solution without PEG served as the control. During this time, aerated nutrient solutions were renewed every other day. After harvest, 30 plants (i.e., 15 PEG-treated plants and 15 control plants) were used to measure root biomass and total N content of *T. ramosissima* and cotton, respectively. The root biomass of each plant of both control and treatment was determined immediately after harvest using a high-precision balance (0.000001) (XP105, Mettler Toledo Inc., Columbus, Ohio), and the number of replicates for root biomass was 15 for both control and for PEG treatments. Total N content in roots was determined using an auto-analyzer (Kjeltec 2300 Analyzer Unit, Foss, Sweden). Following Sun et al. (2016), for reducing error, the roots of *T. ramosissima* and cotton from 15 PEG-treated or control plants were pooled and split to generate three replicates for measuring total N content.

Tamarix ramosissima is the host plant of *C. tubulosa*. To determine whether *C. tubulosa* inoculation affects *T. ramosissima* NO_3^- uptake, an inoculation experiment was prepared. In brief, seeds of *C. tubulosa* were dried at room temperature (25 °C, using an Electro-thermostatic blast oven, and a Shanghai CIMO Medical Instrument Manufacturing Co., LTD, ShangHai, China, DHG-9053BS-III) 1 week prior to inoculation, and then 0.4 g of seeds was mixed with 4 l fine sand (relative humidity 70%). *Tamarix ramosissima* cuttings (~18 cm in length and 1 cm in diameter) were rooted in the sand containing *C. tubulosa* seeds. The sand was covered with transparent film prior to adding the cuttings. Plants were cultivated in a greenhouse (natural light, day/night 28/23 °C, relative humidity: 60–75%) and irrigated every other day with 50 ml of Hoagland's nutrient solution. After about 100 days, some of the roots of *T. ramosissima* were inoculated. In this study, *T. ramosissima* not inoculated with *C. tubulosa* is referred to as 'uninoculated plant', and *T. ramosissima* inoculated with *C. tubulosa* is referred to as 'inoculated plant'. Because not all the roots in an 'inoculated plant' are inoculated with *C. tubulosa*, the root that was inoculated is referred to as 'inoculated plant-inoculated root', and the uninoculated root is referred to as 'inoculated plant-uninoculated root'. The CTZ region of uninoculated plant roots, inoculated plant-inoculated roots and inoculated plant-uninoculated roots was monitored for net NO_3^- fluxes using the NMT technique. Three roots were selected and excised from the root system of each plant, and three to four plants were used for NO_3^- flux analyses.

To understand NO_3^- uptake by the fine roots of *T. ramosissima* and cotton, we monitored the net NO_3^- fluxes at the root surface using the NMT technique, NMT system BIO-IM; Younger USA, LLC, Amherst, MA, USA). The NMT system and its use in detecting net ion flux have been previously described in detail (Han et al. 2015, Shabala et al. 2016). Three fine roots (~1.0 mm in diameter) of *T. ramosissima* and cotton were selected and excised from the root system of each plant in each treatment group. For each treatment, three to seven plants were used for NO_3^- flux analyses.

Uniform seedlings of *T. ramosissima* and cotton (~30–35 cm height) were selected for the stable ^{15}N isotope analysis. The excised roots from both *T. ramosissima* and cotton were used to ^{15}N isotope analysis according to Huang et al. (1992) and Henry and Jefferies (2003). The availability of root material for experiments was limited due to the low growth rate of our study species *T. ramosissima*. Root excision allowed us to pool roots of a large number of cuttings and apportion precise quantities of root to each replicate. Furthermore, *T. ramosissima* was grown from cuttings, but cotton was from seeds. The excised root technique for studying transport into roots was validated in short-term experiments (Huang et al. 1992, Essah et al. 2003) and could mitigate the effect of differential growth background of the test species. Three groups of excised roots (0.3–0.5 g fresh weight for each group) were treated in a one-point application at the concentration of $^{15}NO_3$ indicated (supplied as $Ca(^{15}NO_3)_2$ (99 atom percent ^{15}N), according to Min et al. (2000)); exposure was for 3 h.

Nitrate uptake rate ($^{15}NO_3^-$)

Tamarix ramosissima and cotton seedlings were selected for determination of N-absorption kinetics after pre-culturing for 2 weeks. Plants were then transferred to solutions without N for 2 days prior to influx measurements according to Sun et al. (2016). One of the reasons for restricting the N supply to 2 days prior to influx determinations was that Min et al. (1999) detected appreciable formation of NO_2^- in culture solutions. This probably resulted from the activity of nitrifying/denitrifying organisms carried over from the growth medium before hydroponics. Thus, N starvation provided a means of avoiding NO_2^- accumulation without sacrificing apparent steady-state conditions (Min et al. 1999). Following 2 days of N starvation, excised roots from both *T. ramosissima* and cotton (after exposure to light for 2 h) were transferred to nutrient solutions to which 0, 0.025, 0.05, 0.1, 0.2 and 0.5 mM of $^{15}NO_3^-$ were added. The treatment NO_3^- concentration was modified according to Aslam et al. (2001). Three replicates (0.3–0.5 g fresh weight for each replicate) were used per NO_3^- concentration. After a 3-h treatment (under light), roots were washed, separated, freeze-dried, ground into a powder, and about 0.5 mg of dried powder was subjected to a Thermo Flash 2000 analyzer hyphenated to a Thermo Fisher (Waltham, MA, USA) Delta-V isotope ratio mass spectrometer to determine total N and ^{15}N abundance according to Sun et al. (2016). The formula used was: total ^{15}N amount of the whole plant/dry weight of root/3 h, yielding the amount of ^{15}N taken up per unit weight of root per unit time. Then, the Michaelis–Menten equation was applied to derive the kinetic parameters of V_{max} (the maximum uptake rate) and K_m (the apparent Michalis–Menten constant).

Measurement of net NO_3^- flux with the NMT system

Tamarix ramosissima and cotton seedlings were selected for measurement of NO_3^- flux after pre-culturing for 2 weeks. Plants were N-starved for 2 days without NO_3^- prior to flux analysis. Three fine roots (~1.0 mm in diameter) of *T. ramosissima* and cotton were selected and excised from the root system of each plant in each treatment group. The excised roots were equilibrated in measuring solution for 5 min prior to measurement. The measuring solution contained: 0.1 mM KNO_3, 0.1 mM $MgCl_2$, 0.1 mM NaCl, 0.1 mM $CaCl_2$ and 0.3 mM 2-(*N*-morpholino) ethanesulfonic acid hydrate (MES), pH 6.2, according to Han et al. (2015). The design principles for measuring elements in solution were: (i) Maintain the physiological state of the sample for a short time. Because the test time of sampling did not exceed 20 min, it was not necessary to provide N, trace elements, carbohydrates or vitamins. MES was used to sustain measuring solution pH. (ii) Meet the requirements of the NMT technique. The organic matter and high concentration of some ions affects the sensitivity of the NMT equipment and hence the accuracy of the data, thus the measuring solutions did not contain organic matter, and the concentration of the inorganic ion did not exceed 5 mM. Furthermore, if the measured ion (NO_3^-) concentration was higher, the signal-to-noise ratio was lower, which affected the accuracy of the data. For each treatment, three to seven plants were used for NO_3^- flux analyses using the NMT technique, and the work was conducted at Bapu (Shanghai) Information Technology Co., Ltd. The principle of this method and the instrument are as detailed in Shabala et al. (2016). Briefly, equilibrated roots were transferred to the measuring chamber, a small plastic dish (10-cm diameter), containing 8 ml of fresh measuring solution. After roots were immobilized at the bottom of the dish, a NO_3^--selective ion-selective microelectrode was vibrated in the measuring solution in the different root regions. The four root regions used for measurements of ion flux were defined according to the descriptions of Peterson et al. (1999): white zone (WZ) of main roots (white in color, usually 0–3 cm from the tip) separated into two regions in this study: region 1, 0.5 mm from the root tip and region 2, 20 mm from the root tip; condensed tannin zone (CTZ) of main roots (tan in color, usually 3–5 cm from the tip); and cork zone (CZ) of main roots (brown in color, the primary root region from which lateral roots branched). The background was recorded by vibrating the electrode in measuring solution not containing roots. Ion flux was calculated by Fick's law of diffusion: $J = -D\ (dc/dx)$, where J represents the ion flux (unit: pico moles $cm^{-2}\ s^{-1}$), dc/dx is the ion concentration gradient and D is the ion diffusion constant in the medium. The direction of the flux is derived from Fick's law of diffusion that relates the concentration gradient. The preparation of the NO_3^--selective microelectrode for the assay of NO_3^- fluxes in roots was as follows: pre-pulled and silanized glass micropipettes (XY-DJ-0, Younger USA) were first filled with a backfilling solution (10 mmol l^{-1} KNO_3) to a length of ~1.0 cm from the tip, then the micropipettes were front-filled with 15–50-μm columns of selective liquid ion-exchange (LIX) cocktails (NO_3^- LIX, XY-SJ-NO3, Younger USA) and were inserted in the back of the electrode to make electrical contact with the electrolyte solution. The recording rate of ion flux was one reading per 6 s. YG003-Y05 (Younger USA) was used as the reference electrode.

For the PEG shock treatments, the roots settled on the surface of coverslips in 5 ml of measuring solution, and steady-state NO_3^- fluxes were reported (3–5 min) prior to the PEG treatment. Thereafter, 30% PEG (w/v) stock solution was slowly added to the measuring solution until a final 15% PEG concentration was reached in the solution. Afterwards, the kinetics recording was restarted and continued for 3–5 min. The data measured during the first minute were discarded because of the diffusion effects of the stock addition (Shabala 2000) (in this study, blank measurements, i.e., without root addition, were carried out to exclude the disturbance of stock addition on flux measurements). Transient recordings of the flux kinetics of NO_3^- were measured for specified times.

To test the effect of local PEG shock on average net NO_3^- fluxes in the *T. ramosissima* root, we designed a special test device (see Figure 6a). In brief, a test dish was constructed with a fixed bump partition, and a small hole was opened in the middle of the bump partition. Roots were draped through the hole, and the WZ and CTZ were fixed on either side. The small hole was sealed with vacuum silicone grease to ensure that the measuring solution on both sides did not leak, and thus the WZ and CTZ roots were in their respective testing environment without interference. Five milliliters of measuring solution was added to the both sides of the bump partition. For the local PEG shock treatments, steady-state NO_3^- fluxes were recorded (3–5 min) in the WZ region side prior to PEG treatment. Thereafter, 30% PEG (w/v) solution was slowly added to the WZ (WZ + PEG) or the CTZ (CTZ + PEG) side until the final concentration in the measuring solution reached 15% PEG, while the other components of the measuring solution remained unchanged. Afterwards, the kinetics recording was continued for 3–5 min at the WZ site.

Statistical and graphical analyses

For all experiments, data were statistically analyzed using the SPSS 13.0 program (SPSS, Chicago, IL, USA) and were analyzed using Duncan's multiple-range test, and an independent samples *t*-test. A P-value <0.05 was regarded as significant. Details are as presented in figure legends. Origin 8.0 was used for the generation of graphs. Adobe Photoshop 7.0 was used for photocomposition (layers are revealed by right-clicking on graphs). The graphs were arranged in a sequence and exported as TIFF images. Net flux data were calculated by Mageflux version 1.0, attached to the NMT system (Xu et al. 2006). All data are presented as the means ± standard errors of at least three biological replicate samples.

Results

NO_3^- uptake kinetics in T. ramosissima and cotton

In the concentration range measured there was evidence of classical Michaelis–Menten-style saturation kinetics for NO_3^- flux for both *T. ramosissima* and cotton (Figure 1). However, the two species differed with respect to the concentration ranges of their respective high-affinity transport system for NO_3^- influx. In *T. ramosissima*, NO_3^- influx was saturable up to 0.2 mM $[NO_3^-]$ (Figure 1). Cotton showed a much higher capacity for NO_3^- uptake than *T. ramosissima*: V_{max} for influxes in cotton was approximately three-fold higher than in *T. ramosissima* (Table 1). Further, the K_m for NO_3^- influx was ~10-fold higher in cotton than in *T. ramosissima* (Table 1). This implies that cotton had higher capacity for NO_3^- uptake but *T. ramosissima* had higher NO_3^- affinity.

Locations of maximal net NO_3^- fluxes

To understand the N uptake of fine roots, NMT was employed, and net NO_3^- fluxes were monitored in different regions of the WZ of roots (region 1, 0.5 mm from the root tip; region 2, 20 mm from the root tip) (Figure 2a). This technique allowed the determination of the maximal net uptake of roots in *T. ramosissima* and cotton. In the measuring solution, there were significantly different net NO_3^- influxes in the two root regions of cotton (Figure 2b and c). The maximal net uptake rate of NO_3^- was ~50 pmol m^{-2} s^{-1} for region 1, and 220 pmol m^{-2} s^{-1} for region 2 of cotton roots (Figure 2c). However, no significant NO_3^- influx signals were observed in both the WZ root region

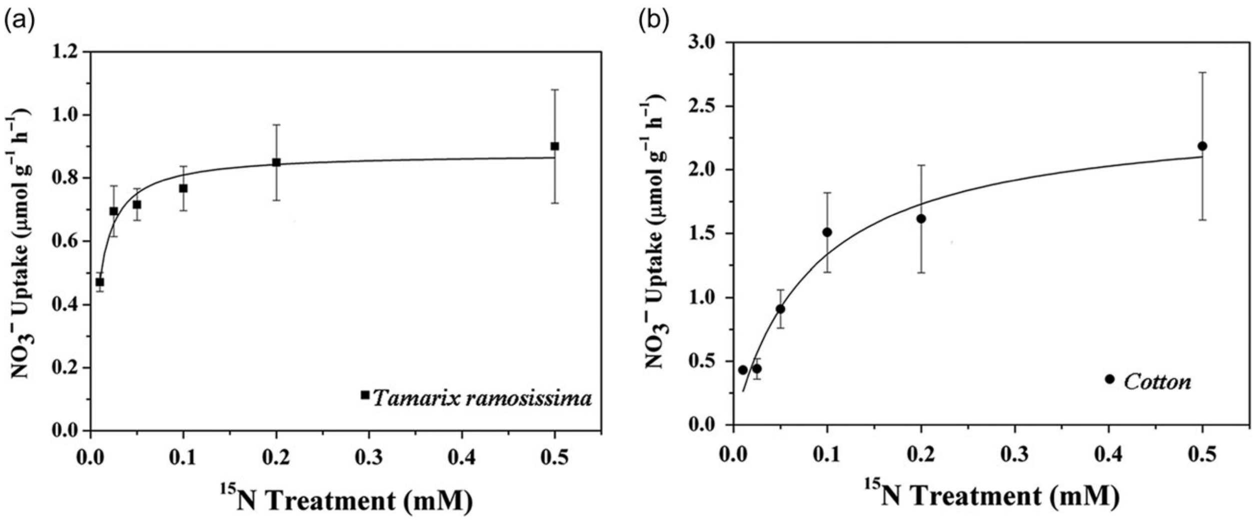

Figure 1. $^{15}NO_3^-$ uptake in roots of *T. ramosissima* (a) and cotton (b) seedlings. Values shown are the means ± SD of three replicates, and are fitted to the Michaelis–Menten equation.

and CTZ (50 mm from the root tip) and the CZ region of *T. ramosissima* (Figure 2b–d). Clearly, cotton seedlings showed a much higher capacity for NO_3^- uptake than *T. ramosissima* seedlings, consistent with the observations of $^{15}NO_3^-$ uptake kinetics.

Effect of C. tubulosa *inoculation on NO_3^- fluxes of* T. ramosissima

Tamarix ramosissima is the host plant of *C. tubulosa*. To determine whether *C. tubulosa* inoculation affects *T. ramosissima* NO_3^- uptake, we monitored net NO_3^- fluxes in the CTZ region of inoculated plants using the NMT technique. We found that there were no remarkable changes in flux signals between inoculated and uninoculated plants (Figure 3).

Effect of PEG-simulated drought stress on NO_3^- fluxes

Following exposure to PEG-induced water stress, the net flux of NO_3^- varied significantly between *T. ramosissima* and cotton. Upon PEG stimulation, NO_3^- influx of cotton switched to efflux, and there was an obvious efflux signal of NO_3^-, with a substantive peak of ~400 pmol m^{-2} s^{-1}, in root region 2 (20 mm from

Table 1. Kinetics parameters of NO_3^--N uptakes by *T. ramosissima* and cotton (means ± SD, $n = 3$). V_{max} and K_m were determined by a non-linear curve-fitting model (Michaelis–Menten kinetics). DW: dry weight.

Species	Kinetic equation	R^2	K_m (μmol l^{-1})	V_{max} (μmol g^{-1} DW h^{-1})
T. ramosissima	$y = 0.878 * x/(0.00852 + x)$	0.9334	8.52 ± 1.51	0.878 ± 0.025
Cotton	$y = 2.45 * x/(0.0831 + x)$	0.9253	83.1 ± 25.6	2.45 ± 0.265

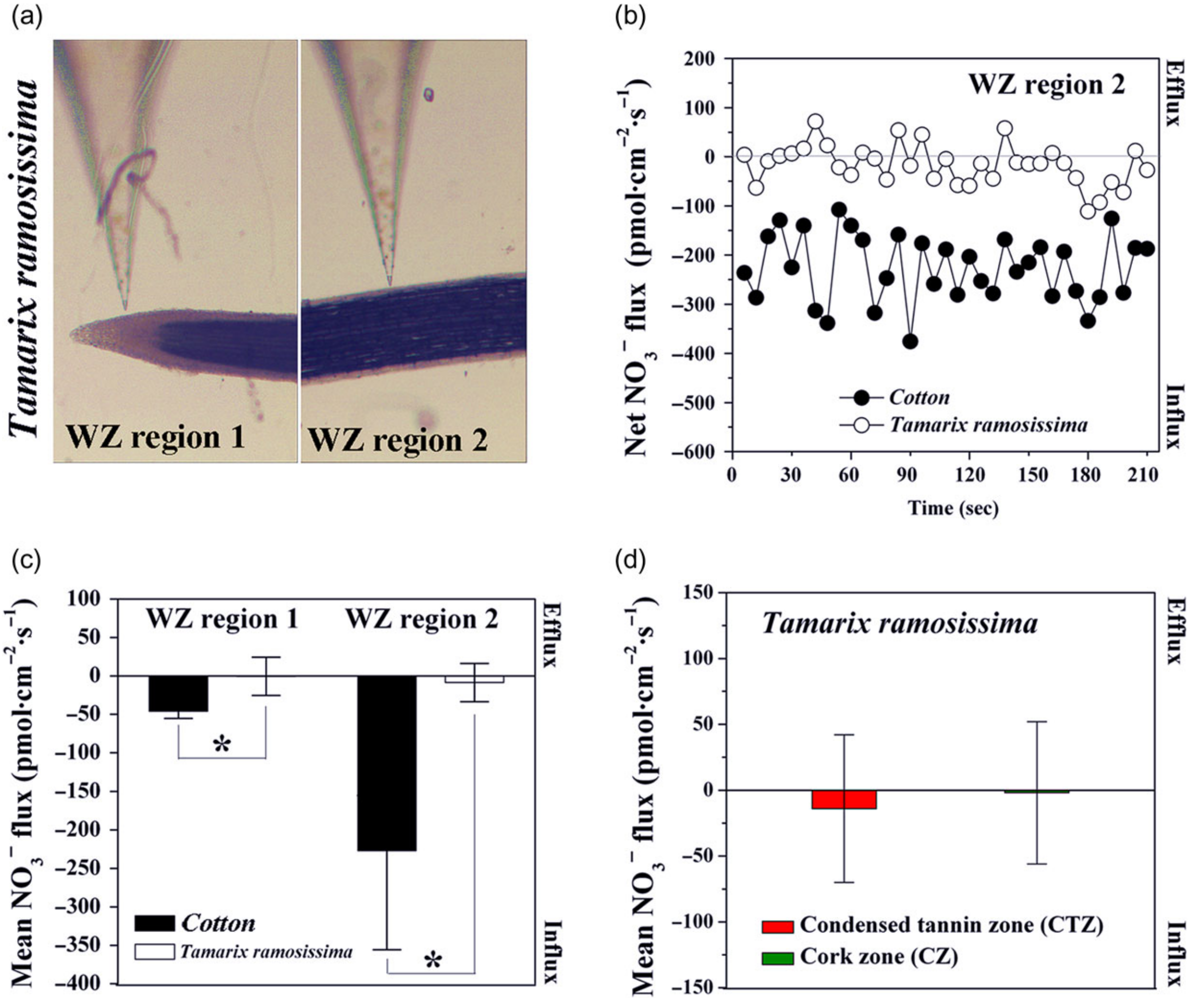

Figure 2. Net NO_3^- flux in the roots of *T. ramosissima* and cotton. Negative values correspond to net influxes, while positive values indicate net effluxes. (a) *Tamarix ramosissima* root WZ. White zone region 1, 0.5 mm from the root tip; WZ region 2, 20 mm from the root tip. (b) Net NO_3^- flux in the WZ region 1 and 2 of *T. ramosissima* and cotton. A continuous flux recording was obtained for each root in corresponding measuring solutions. (c) Mean net fluxes of NO_3^- in (b). Data indicate the means ± SD ($n = 5$). Columns labeled with * indicate significant difference at $P < 0.05$. (d) Mean net fluxes of NO_3^- in the CTZ and the CZ of *T. ramosissima* root. Data indicate the means ± SD ($n = 4$–7).

the root tip) (Figure 4a and c). However, net NO_3^- flux in *T. ramosissima* exhibited some interesting differences. There were no significant NO_3^- influx signals observed in WZ region 2 (20 mm from the root tip) of *T. ramosissima* in the zero-PEG control (Figure 4b and c). The PEG shock significantly enhanced NO_3^- influx in root WZ region 2 and resulted in a substantive peak of ~300 pmol m^{-2} s^{-1} influx compared with the mock condition (Figure 4b and c). We further examined whether *C. tubulosa* inoculation affects *T. ramosissima* NO_3^- uptake under PEG treatment. Addition of PEG switched net NO_3^- flux to significant influx in the inoculated-root CTZ region (Figure 5).

We further asked whether PEG regulation of NO_3^- fluxes at the root surface may be changed by direct PEG contact (Figure 6a). Addition of PEG to the CTZ region (50 mm from the root tip) did not result in changes of NO_3^- fluxes in WZ region 2 (20 mm from the root tip) in *T. ramosissima* (Figure 6b). When PEG was supplied to WZ region 1 (0.5 mm from the root tip), NO_3^- fluxes in WZ region 2 (20 mm from the root tip) were also unchanged in *T. ramosissima* (data not shown).

Changes in root total N content and biomass under PEG-induced water stress

Under control conditions (without PEG treatment), total root N content of cotton was higher than in *T. ramosissima* (Figure 7). Root N content was significantly suppressed by PEG-induced water stress in cotton (Figure 7), consistent with the NO_3^- uptake of cotton seedlings being significantly decreased by PEG treatment (Figure 4a and c). However, N content was slightly increased in *T. ramosissima* roots under PEG treatment (Figure 7).

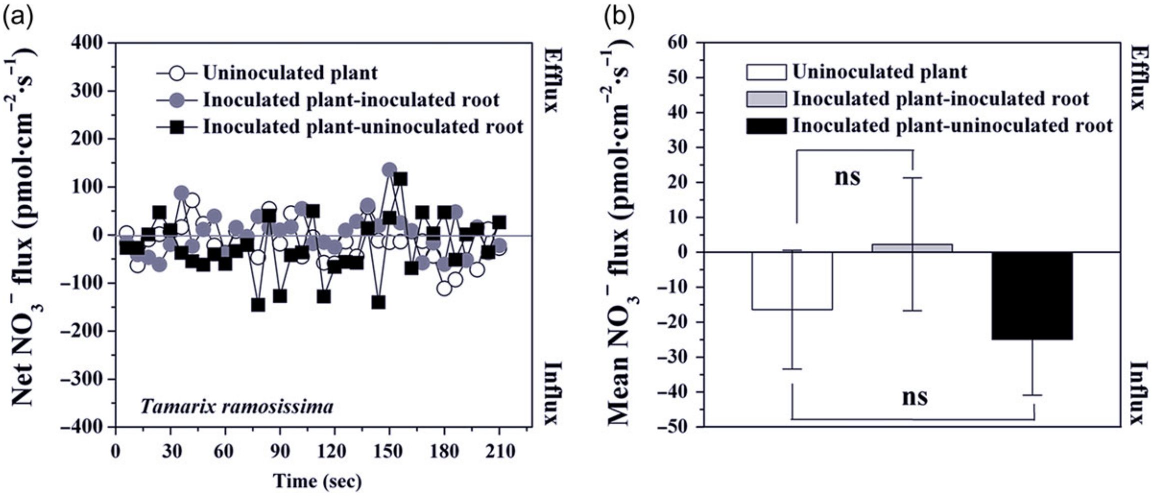

Figure 3. Net NO_3^- flux in the roots of *C. tubulosa*-inoculated and -uninoculated *T. ramosissima*. (a) Net NO_3^- flux in the root the CTZ region of *C. tubulosa*-inoculated and -uninoculated *T. ramosissima*. A continuous flux recording was obtained for each root in corresponding measuring solutions. (b) Mean net fluxes of NO_3^- in (a). Data indicate means ± SD ($n = 3$–4). ns, not significant.

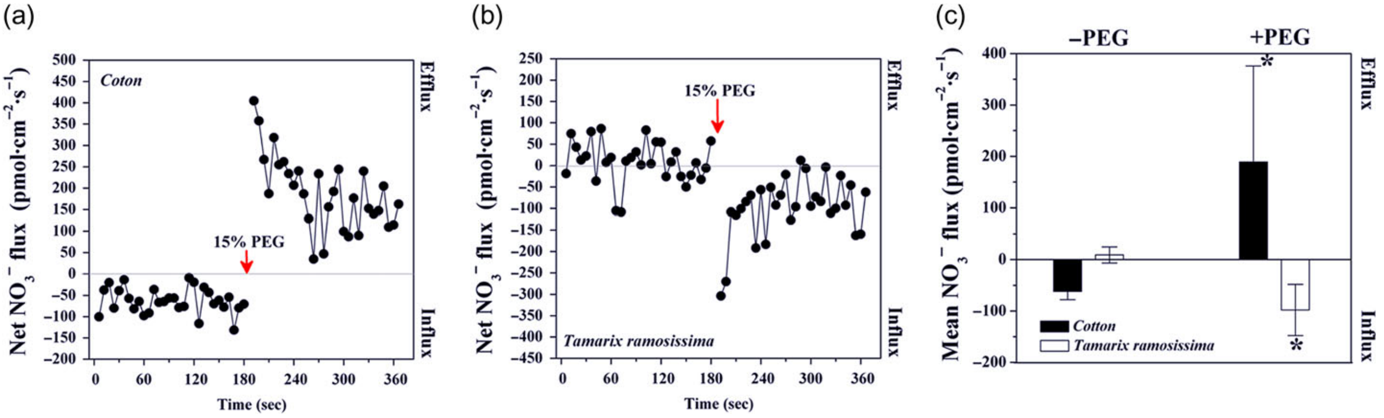

Figure 4. Transient NO_3^- kinetics in response to 15% PEG shock in the root WZ region 2 of *T. ramosissima* and cotton. (a) Effects of 15% PEG (indicated by the arrow) on net NO_3^- fluxes at the root WZ region 2 of the cotton. (b) Effects of 15% PEG on net NO_3^- fluxes at the root WZ region 2 of *T. ramosissima*. (c) Mean values of NO_3^- fluxes from (a) and (b). Asterisk (*) denotes statistical significance between −PEG and +PEG treatment of *T. ramosissima* and cotton, respectively (independent samples *t*-test, $P < 0.05$, $n = 5$–6). Values shown are the means ± SD.

Since N status can influence the drought resistance of plants (Zong and Shangguan 2014), we examined the consequences of longer-term exposure to PEG. After 1 week of exposure to PEG, PEG-treated cotton plants exhibited root growth inhibition, resulting in decreased biomass compared with the control (Figure 8), whereas there was a comparable nonsignificant decrease in root biomass of *T. ramosissima* under the same treatment conditions (Figure 8).

Discussion

Characteristics of the NO_3^- kinetic parameters

Among the mechanisms plants have evolved to deal with nutrient-poor conditions, adaptations in root interception and primary acquisition mechanisms are critical. In terms of the latter, differences in kinetic parameters often have ecological significance. The differential enforcement by natural selection of evolutionary ‘strategies’ determined the trajectory of K_m over evolutionary time (Growly 1975). In high-nutrient environments, K_m can become large; in low-nutrient environments, K_m can become small, and substantially lower K_m values do appear to reveal an adaptation to a nutrient-poor environment (Cacco et al. 1980). For example, K_m values for NO_3^- uptake were 153 μM for lodgepole pine and 11 μM for trembling aspen, respectively, and aspen was capable of thriving on low NO_3^-; by contrast, kinetic parameters for N acquisition in lodgepole pine identify it as a specialist species particularly well adapted to high soil-N concentrations (Min et al. 2000). In the current study, a comparison with cotton, a major commercial crop in Xinjiang, China, revealed that *T. ramosissima* displays a significantly lower K_m (8.5 μM) for NO_3^- influx, using an excised-root technique (Table 1), suggesting a higher affinity for the NO_3^- substrate. K_m values for NO_3^- uptake in the literature for tree species range from 17 μM for Douglas-fir (Kamminga-van Wijk and Prins 1993) to 100 μM for white spruce (Kronzucker et al. 1995*b*), 200 μM for Norway spruce (Peuke and Tischner 1991) and 153 μM for lodgepole pine (Min et al. 2000). These results show that *T. ramosissima* has a higher affinity for NO_3^- than many previously examined trees. While these studies used different methods for both experimental and statistical analysis from those used in the current study, the substantially lower K_m does appear to reveal an adaptation to a nutrient-poor environment (Cacco et al. 1980). The rate of NO_3^- uptake was not high, especially when compared with that of cotton (Table 1; Figure 1). This must be viewed in the context that *T. ramosissima* growth is relatively slow and, thus, growth demand is also low. A combination of low K_m and low growth rate is often more conducive to survival and competition in nutrient-poor environments (Pettersson and Jensen 1983, Min et al. 2000). The commonly used excised-root technique, then, can yield results of much greater precision than is attainable with individual sets of entire seedlings (Huang et al. 1992, Essah et al. 2003), root excision allows for the pooling of roots from a large number of cuttings and precise quantities of root can be apportioned to each replicate (Epstein et al. 1962), and effects of differential growth background of test species maybe also attenuated. Experiments with entire plants grown for extended periods rate high in their probable relevance to real-life plant nutrition, but low in precision and the ability to provide results amenable to mechanistic interpretations. Work on whole plants over extended periods throughout the day is also complicated by diurnal cycling, and the fact that light is known to strongly regulate NO_3^- uptake in particular (Delhon et al. 1996, Lejay et al. 1999, 2003, Ono et al. 2000, Lillo 2008).

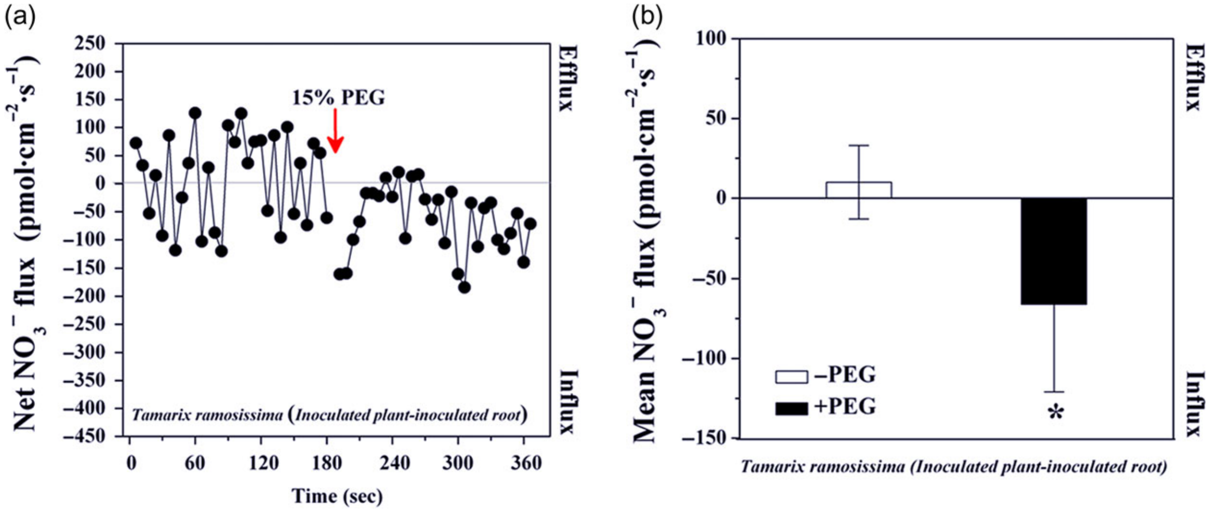

Figure 5. Transient NO_3^- kinetics in response to 15% PEG shock in the root CTZ of *C. tubulosa*-inoculated *T. ramosissima*. (a) Effects of 15% PEG (indicated by the arrow) on net NO_3^- fluxes at the root CTZ of *C. tubulosa*-inoculated *T. ramosissima*. (b) Mean values of NO_3^- fluxes from (a). Asterisk (*) denotes statistical significance between −PEG and +PEG treatment (independent samples *t*-test, $P < 0.05$, $n = 4$). Values shown are the means ± SD.

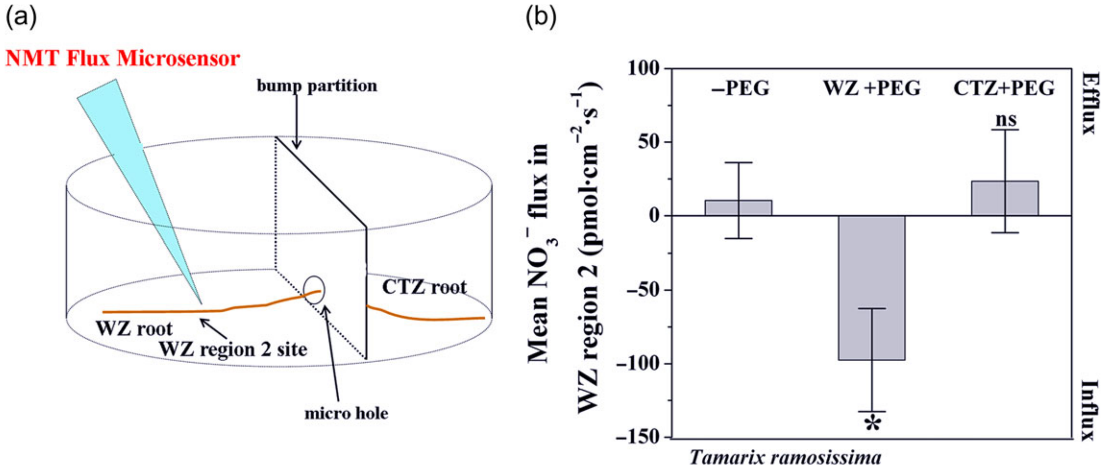

Figure 6. Effect of local PEG shock on net NO_3^- flux in the roots of *T. ramosissima*. (a) Schematic diagram of local PEG shock. The blue triangle represented the NMT flux microsensor. (b) The effect of local 15% PEG shock on average net NO_3^- fluxes in the root WZ region 2. Asterisk (*) denotes statistical significance between −PEG and +PEG treatment; ns, not significant (independent samples *t*-test, $P < 0.05$). Values shown are the means ± SD

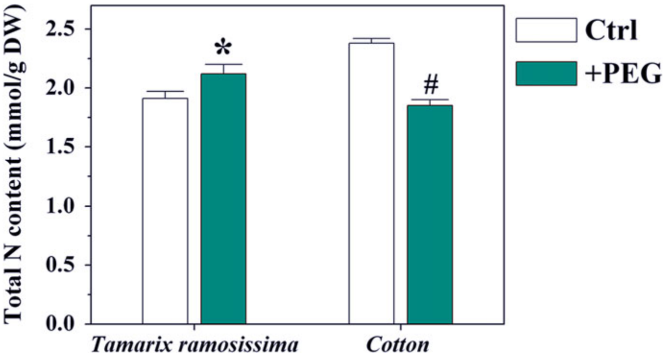

Figure 7. Effect of PEG treatment on root total N content of *T. ramosissima* and cotton. *Tamarix ramosissima* and cotton were treated with 15% PEG for 7 days and the root total N content was measured. Values shown are the means ± SD of three replicates. Asterisk (*) and octothorpe (#) denote statistical significance between control and +PEG treatment in *T. ramosissima* and cotton, respectively ($P < 0.05$). Ctrl: without PEG treatment; +PEG: 15% PEG treatment. DW: dry weight.

Characteristics of the NO_3^- fluxes along the root

A previous study had suggested that the white (WZ) and condensed tannin (CTZ) zones of woody plant roots have the highest flux of NO_3^- (Hawkins et al. 2014). Indeed, seedlings of some woody plants show the highest net NO_3^- uptake between 5 and 20 mm from root tips (Zhang et al. 2014, Meng et al. 2016). For example, the maximum net NO_3^- influx (112 pmol m^{-2} s^{-1}) in *Populus simonii* occurred 15 mm from the root tip (Zhang et al. 2014). In our study, the net NO_3^- influx was also found to be higher 20 mm rather than 0.5 mm from the root tip of cotton (Figure 2c), but there was no significant net NO_3^- influx from the WZ to the CZ root regions of *T. ramosissima* (Figure 2b–d). These results suggest that *T. ramosissima* has different NO_3^- absorption characteristics from other woody plants. Different NO_3^- absorption characteristics reflect differences in soil habitat, expression of NO_3^- transporters or genes responsible for these transporters, and in post-transcriptional regulation and internal feedback loops (Kronzucker et al., 1995*a*). For example, *Arabidopsis AtNRT1.1* is mainly expression in the root (Tsay et al. 1993, Wang et al. 2012); however, tomato has two homologous genes of *Arabidopsis AtNRT1.1*: *LeNRT1-1* and *LeNRT1-2* (Lauter et al. 1996). *LeNRT1-1* is mainly expressed in the root, and *LeNRT1-2* is especially expressed in root hairs (Lauter et al. 1996).

Characteristics of NO_3^- fluxes under PEG-induced water stress

Arid and semi-arid ecosystems are frequently co-limited by the availability of both soil water and N (Zhang et al. 2013). Few studies have investigated the physiological mechanisms that allow woody plants to respond to drought by regulating N influx and efficiency (Gessler et al. 2017, Luo and Luo 2017). Drought can inhibit plant growth, and this inhibition is often accompanied by a decrease in tissue N content under drought (Shi et al. 2017). Impaired N uptake as well as lowered tissue nutrient content has been widely observed in drought-susceptible plants during drought episodes (Fotelli et al. 2002). Consistent with this, biomass and N content of cotton was significantly decreased under PEG-induced water stress in this study (Figures 7 and 8). Our data suggest that the decrease in cotton-root N content may partly result from PEG-stimulated NO_3^- efflux (Figure 4a and c). By contrast, under PEG-induced water stress, net NO_3^- fluxes in *T. ramosissima* switched to influx, and did not display periods of net efflux (Figure 4b and c), and thus the ability to preserve N is more prominent than in cotton (Figure 7), mitigating water stress-induced inhibition of seedling growth (Tran et al. 2014, Figure 8). The characteristics of NO_3^- acquisition and access to, or depletion

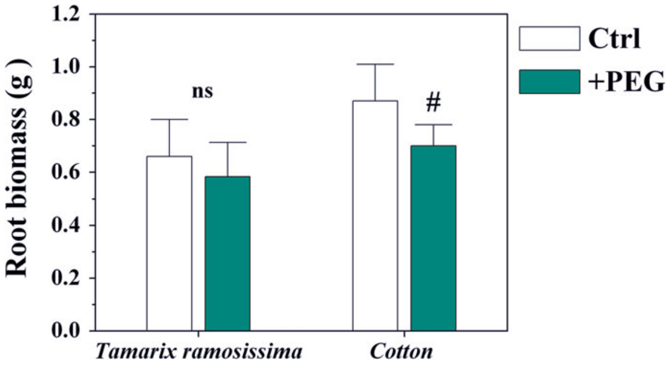

Figure 8. Effect of PEG treatment on root biomass of *T. ramosissima* and cotton. *Tamarix ramosissima* and cotton were treated with 15% PEG for 7 days and the root biomass was measured. Octothorpe (#) denotes statistical significance between control and +PEG treatment. ns, not significant (independent samples *t*-test, $P < 0.05$, $n = 15$). Values shown are the means ± SD. Ctrl: without PEG treatment; +PEG: 15% PEG treatment.

of, internal N reserves during drought stress of *T. ramosissima* are clearly different from some other woody plants that have been reported, e.g., *Catalpa bungei* and *Populus simonii*, which show significantly decreased NO_3^- uptake and tissue content under drought stress (Meng et al. 2016, Shi et al. 2017). Nutrient availability during drought has impacts on survival that are distinct from nutrient availability before drought, and low nutrient uptake during drought should promote negative impacts on plant survival (Gessler et al. 2017). It was suggested that the increased NO_3^- absorption rate induced by drought stimulation should rapidly increase N accumulation and thus enhance prolonged drought tolerance of *T. ramosissima*. Drought has been shown to suppress the expression of genes encoding NO_3^- transporters as well as NO_3^- influx in *Malus prunifolia*, and thus reduce root N content and biomass (Huang et al. 2018). Shi et al. (2017) suggested that the extent of abscisic acid inducement upon drought was elevated by sufficient N. We also show that the PEG-triggered NO_3^- influx in *T. ramosissima* requires the root to be in direct contact with external PEG (Figure 6b). In addition to the effects of PEG, regulatory effects by other environmental stresses, such as high ammonium (Li et al. 2010) or iron (Zhang et al. 2018), on nutrient ion flux, have also been reported to be local effects, requiring direct root contact with the stimulatory or suppressive agent. Because NO_3^- influx is an energy-intensive process (Britto and Kronzucker 2006), we suspect that this kind of point-to-point response to water stress may be more conducive to conserving energy and to long-term drought resistance, especially in long-lived woody species such as *T. ramosissima*.

Characteristics of NO_3^- fluxes following inoculation with the parasitic angiosperm C. tubulosa

Inoculation with ectomycorrhizal fungi has been suggested to present a potential strategy for enhancing the performance of, and ensuring biomass production by, woody species under environmental stress (Luo et al. 2009). Ectomycorrhizal associations failed to reduce tissue concentrations of Na^+ in NaCl-treated trembling aspen (*Populus tremuloides*, Yi et al. 2008). Li et al. (2012) suggested that the net K^+ flux of *Populus canescens* was not affected by *Paxillus involutus* (an ectomycorrhizal fungus) colonization under normal conditions. Parasitic plants may have a very strong impact on crops cultivation in different areas of the world (Parker 2009, Pignone and Hammer 2016), and some of these plants can cause severe damage. Previous studies clearly show that parasitic angiosperms (e.g., *Striga gesnerioides*, *Cuscuta reflexa*) can inhibit the growth of host plants (Hibberd et al. 1996, Jeschke et al. 1997). *Tamarix ramosissima* is the major host plant of the parasitic angiosperm *C. tubulosa*, which is a profitable medicinal plant in Xinjiang, China (Zhang and Zhang 2012). However, whether *C. tubulosa* parasitism affects the primary process of N acquisition in the host plant is not known, and was investigated here in *T. ramosissima* infected with *C. tubulosa*. The results show that there were no marked changes in ion flux signals in *C. tubulosa*-inoculated plants compared with uninoculated *T. ramosissima* (Figure 3). We further tested whether *C. tubulosa* inoculation affects NO_3^- uptake in *T. ramosissima* roots under PEG shock. Addition of PEG switched net NO_3^- flux to significant influx in the inoculated root (Figure 5), similar to what was observed in the absence of inoculation. The results suggest that the increased NO_3^- absorption rate induced by drought stimulation is retained in *C. tubulosa*-inoculated *T. ramosissima*.

Conclusions

In conclusion, our study provides insight into NO_3^- uptake and the effects of *C. tubulosa* inoculation in roots of *T. ramosissima* under control conditions and in response to PEG-induced water stress. We conclude that the excellent growth of *T. ramosissima* on nutrient-poor and drought-afflicted soils relates to key distinctive features of its nutrition acquisition mechanisms, as follows:

- *Tamrix ramosissima* has a higher affinity for NO_3^- than many conifers and cotton (used here as a model species). A lower K_m does appear to indicate a higher affinity for the substrate (Growly 1975), and *T. ramosissima* displays a significantly lower K_m (8.5 μM) for NO_3^- influx than cotton and than reported in some previously studied conifers.
- The nutrient uptake rates are not high under non-arid conditions (Table 1; Figure 2), but the growth of *T. ramosissima* is relatively slow (Xiao et al. 2005), and thus the demand for nutrient is also low.
- As suggested in previous studies (Huang et al. 2018), PEG can significantly inhibit net NO_3^- influxes and reduce the root N content. Consistently, following PEG treatment, NO_3^- influx in cotton switched to efflux and reduced root N content (Figures 4a and c, 7). However, under PEG-induced water stress, net NO_3^- fluxes of *T. ramosissima* showed influx

stimulation (Figure 4b and c) and, thus, enhanced ability for conserving N (Figure 7).

- The effect of PEG on net NO_3^- flux in roots is highly spatially confined (Figure 6), conserving energy under stress conditions. Because NO_3^- influx is an energy-intensive process (Britto and Kronzucker 2006), we hypothesize that this kind of point-to-point response to water stress may be more conducive to conserving energy and to long-term drought resistance, especially in long-lived woody species such as *T. ramosissima*.
- Despite the fact that parasitic angiosperms have negative effects on host plants, the response of increased net NO_3^- influx to drought stimulation was also found in *C. tubulosa*-inoculated *T. ramosissima* plants (Figure 5), suggesting that parasitic relations between *C. tubulosa* and *T. ramosissima* do not eliminate the superior NO_3^- absorption characteristics of *T. ramosissima* under drought.

Our findings are valuable for understanding NO_3^- uptake mechanisms in the context of adaptation to drought and will provide guidelines for silviculture and breeding of *T. ramosissima* under coupled conditions of soil drought and N deficiency. Our study lays the physiological foundation for examinations at the molecular level, whose goals should be the provision of targeted tools for enhancing the efficiency of N use and drought tolerance in arid environments. Further research on the highly efficient NO_3^- acquisition mechanism of *T. ramosissima* under drought might provide important new clues for promoting NO_3^- uptake of other crops and trees in response to drought stress. Applications of PEG, while excellent for detailed mechanistic studies in hydroponic systems, ultimately simulate an osmotic stress, and, therefore, future research on drought in soils, and work on mature trees, to reveal the mechanism(s) by which *T. ramosissima* adapts to changes in water status and N availability in the field, will be needed.

Acknowledgments

We thank Abdul Saimaiti for help to collect the seeds of *C. tubulosa* and cutting of *T. ramosissima*.

Conflict of interest

The authors declare no conflict of interest.

Funding

This work was supported by the National Natural Science Foundation of China (31430095), the National Key R&D Program of China (2017YFD0200103), the Scientific Research Project of Wuxi Enterprise Academician Joint Research Site (CYR1607), the Enterprise Academician Workstation Foundation (BC20150003Z), the Chinese Academy of Sciences Innovation Program (CAS ISSASIP1604) and the University of Melbourne.

Authors' contributions

L.Z. and G.L. executed the experiments, interpreted data and generated figures, and was the major writer of the manuscript. W.S was involved in the design of experiments, analysis and interpretation of the data, and assisted in writing of the manuscript. H.J.K. assisted in discussion and the writing of the manuscript. G.D., M.W. and D.D. assisted in discussion.

References

Aslam M, Travis RL, Rains DW (2001) Inhibition of net nitrate uptake by ammonium in Pima and Acala cotton roots. Crop Sci 41:1130–1136.

Babst BA, Coleman GD (2018) Seasonal nitrogen cycling in temperate trees: transport and regulatory mechanisms are key missing links. Plant Sci 270:268–277.

Britto DT, Kronzucker HJ (2006) Futile cycling at the plasma membrane: a hallmark of low-affinity nutrient transport. Trends Plant Sci 11: 529–534.

Cacco G, Ferrari C, Saccomani M (1980) Pattern of sulfate uptake during root elongation in maize: its correlation. Physiol Plant 48:375–378.

Cleverly J, Smith S, Sala A, Devitt D (1997) Invasive capacity of *Tamarix ramosissima* in a mojave desert floodplain: the role of drought. Oecologia 108:583–595.

Coskun D, Britto DT, Shi WM, Kronzucker HJ (2017) How plant root exudates shape the nitrogen cycle. Trends Plant Sci 22:661–673.

Crawford NM, Forde BG (2002) Molecular and developmental biology of inorganic nitrogen nutrition. In: Meyerowitz E, Somerville C (eds) The Arabidopsis book. American Society of Plant Biologists, Rockville, MD, pp 1–25.

Delhon P, Gojon A, Tillard P, Passama L (1996) Diurnal regulation of NO3- uptake in soybean plants IV. Dependence on current photosynthesis and sugar availability to the roots. J Exp Bot 47:893–900.

Epstein E, Rains DW, Schmid WE (1962) Course of cation absorption by plant tissue. Science 136:1051–1052.

Essah PA, Davenport R, Tester M (2003) Sodium influx and accumulation in *Arabidopsis*. Plant Physiol 133:307–318.

Fotelli M, Rennenberg H, Gessler A (2002) Effects of drought on the competitive interference of an early successional species (*Rubus fruticosus*) on *Fagus sylvatica* L. seedlings: ^{15}N uptake and partitioning, responses of amino acids and other N compounds. Plant Biol 4: 311–320.

Gessler A, Schaub M, McDowell NG (2017) The role of nutrients in drought-induced tree mortality and recovery. New Phytol 214: 513–520.

Gries D, Foetzki A, Arndt SK, Bruelheide H, Thomas FM, Zhang XM, Runge M (2005) Production of perennial vegetation in an oasis-desert transition zone in NW china-allometric estimation, and assessment of flooding and use effects. Plant Ecol 181:23–43.

Growly PH (1975) Natural selection and the Michaelis constant. J Theor Biol 50:471–475.

Han YL, Liu QL, Gu JD, Gong JM, Guan CY, Lepo JE, Rong XM, Song HX, Zhang ZH (2015) V-ATPase and V-PPase at the tonoplast affect NO_3^- content in *Brassica napus* by controlling distribution of NO_3^- between the cytoplasm and vacuole. J Plant Growth Regul 34:22–34.

Hawkins BJ, Robbins S, Porter RB (2014) Nitrogen uptake over entire root systems of tree seedlings. Tree Physiol 34:334–342.

Hejnak V, Tatar O, Atasoy GD, Martinkova J, Celen AE, Hnilicka F, Skalicky M (2015) Growth and photosynthesis of Upland and Pima cotton: response to drought and heat stress. Plant Soil Environ 61:507–514.

Henry HAL, Jefferies RL (2003) Interactions in the uptake of amino acids, ammonium and nitrate ions in the Arctic salt-marsh grass, *Puccinellia phryganodes*. Plant Cell Environ 26:419–428.

Hernández I, Peralta G, Pérez-Lloréns JL, Vergara JJ, Niell FX (1997) Biomass and dynamics of growth of Ulva species in Palmones River Estuary. J Phycol 33:764–772.

Hibberd JM, Quick WP, Press MC, Scholes JD (1996) The influence of the parasitic angiosperm *Striga gesnerioides* on the growth and photosynthesis of its host, *Vigna unguiculata*. J Exp Bot 47:507–512.

Hoagland DR, Arnon DI (1950) The water-culture method for growing plants without soil. Circular. California Agriculture Station, Berkeley.

Houlton BZ, Sigman DM, Schuur EAG, Hedin LO (2007) A climate-driven switch in plant nitrogen acquisition within tropical forest communities. Proc Natl Acad Sci USA 104:8902–8906.

Huang LL, Li MJ, Zhou K, Sun TT, Hu LY, Li CY, Ma FW (2018) Uptake and metabolism of ammonium and nitrate in response to drought stress in *Malus prunifolia*. Plant Physiol Biochem 127:185–193.

Huang Z, Yan X, Jalil A, Norlyn JD, Epstein E (1992) Shortterm experiments on ion transport by seedlings and excised roots. Plant Physiol 100:1914–1920.

Jeschke WD, Baig A, Hilpert A (1997) Sink-stimulated photosynthesis, increased transpiration and increased demand-dependent stimulation of nitrate uptake: nitrogen and carbon relations in the parasitic association *Cuscuta reflexa-Coleus blumei*. J Exp Bot 48:915–925.

Jiang Y, Tu PF (2009) Analysis of chemical constituents in *Cistanche* species. J Chromatogr A 1216:1970–1979.

Kamminga-van Wijk C, Prins HBA (1993) The kinetics of NH_4^+ and NO_3^- uptake by Douglas fir from single N-solutions and from solutions containing both NH_4^+ and NO_3^-. Plant Soil 151:91–96.

Kronzucker HJ, Glass ADM, Siddiqi MY (1995*a*) Nitrate induction in spruce: an approach using compartmental analysis. Planta 196: 683–690.

Kronzucker HJ, Siddiqi MY, Glass ADM (1995*b*) Kinetics of NO_3^- influx in spruce. Plant Physiol 109:319–326.

Kronzucker HJ, Siddiqi MY, Glass ADM (1997) Conifer root discrimination against soil nitrate and the ecology of forest succession. Nature 385:59–61.

Kronzucker HJ, Siddiqi MY, Glass ADM, Kirk GJD (1999) Nitrate-ammonium synergism in rice: a subcellular analysis. Plant Physiol 119: 1041–1046.

Kronzucker HJ, Siddiqi MY, Glass ADM, Britto DT (2003) Root ammonium transport efficiency as a determinant in forest colonization patterns: an hypothesis. Physiol Plant 177:164–170.

Lauter FR, Ninnemann O, Bucher M, Riesmeier JW, Frommer WB (1996) Preferential expression of an ammonium transporter and of two putative nitrate transporters in root hairs of tomato. Proc Natl Acad Sci USA 93:8139–8144.

Lejay L, Tillard P, Lepetit M, Olive Francesc D, Filleur S, Daniel-Vedele F, Gojon A (1999) Molecular and functional regulation of two NO_3^- uptake systems by N- and C-status of *Arabidopsis* plants. Plant J 18: 509–519.

Lejay L, Gansel X, Cerezo M, Tillard P, Muller C, Krapp A, Von Wiren N, Daniel-Vedele F, Gojon A (2003) Regulation of root ion transporters by photosynthesis: functional importance and relation with hexokinase. Plant Cell 15:2218–2232.

Li CC, Li QR, Qiao N, Xu XL, Li QK, Wang HM (2015) Inorganic and organic nitrogen uptake by nine dominant subtropical tree species. iForest 9:253–258.

Li J, Bao S, Zhang Y et al. (2012) *Paxillus involutus* strains MAJ and NAU mediate K^+/Na^+ homeostasis in ectomycorrhizal *Populus*×*canescens* under sodium chloride stress. Plant Physiol 159:1771–1786.

Li Q, Li BH, Kronzucker HJ, Shi WM (2010) Root growth inhibition by NH_4^+ in *Arabidopsis* mediated by the root tip and is linked to NH_4^+ efflux and GMPase activity. Plant Cell Environ 33:1529–1542.

Lillo C (2008) Signalling cascades integrating light-enhanced nitrate metabolism. Biochem J 415:11–19.

Liu M, Li CC, Xu XL, Wanek W, Jiang N, Wang HM, Yang XD (2017) Organic and inorganic nitrogen uptake by 21 dominant tree species in temperate and tropical forests. Tree Physiol 37:1515–1526.

Liu M, Xu FZ, Xu XL, Wanek W, Yang XD (2018) Age alters uptake pattern of organic and inorganic nitrogen by rubber trees. Tree Physiol. doi: 10.1093/treephys/tpy031

Liu XP, Fan YY, Long JX, Wei RF, Kjelgren R, Gong CM, Zhao J (2013) Effects of soil water and nitrogen availability on photosynthesis and water use efficiency of *Robinia pseudoacacia* seedlings. J Environ Sci 25:585–595.

Luo X, Zhu XX, Du Y, Guo YH (2011) Study on the nitrogen-absorbing characters in different root parts of *Tamarix chinensis* Lour. Chinese Agr Sci Bull (in Chinese) 27:66–69.

Luo Z, Janz D, Jiang X, Göbel C, Wildhagen H, Tan Y, Rennenberg H, Feussner I, Polle A (2009) Upgrading root physiology for stress tolerance by ectomycorrhizas: insights from metabolite and transcriptional profiling into reprogramming for stress anticipation. Plant Physiol 151: 1902–1917.

Luo ZB, Luo J (2017) Uncovering the physiological mechanisms that allow nitrogen availability to affect drought acclimation in *Catalpa bungei*. Tree Physiol 37:1453–1456.

Meng S, Zhang CX, Su L, Li YM, Zhao Z (2016) Nitrogen uptake and metabolism of *Populus simonii* in response to PEG-induced drought stress. Environ Exp Bot 123:78–87.

Min J, Dong GQ, Xie WM, Li YL, Ji RT, Shi WM (2018) Soil nutrients status in *Tamarisk* host woodland of *Cistanche tubulosa*. Soils (in Chinese) 50:73–78.

Min XJ, Siddiqi MY, Guy RD, Glass ADM, Kronzucker HJ (1999) A comparative study of fluxes and compartmentation of nitrate and ammonium in early-successional tree species. Plant Cell Environ 22: 821–830.

Min XJ, Siddiqi MY, Guy RD, Glass ADM, Kronzucker HJ (2000) A comparative kinetic analysis of nitrate and ammonium influx in two early-successional tree species of temperate and boreal forest ecosystems. Plant Cell Environ 23:321–328.

Money NP (1989) Osmotic pressure of aqueous polyethylene glycols: relationship between molecular weight and vapor pressure deficit. Plant Physiol 91:766–769.

Näsholm T, Kielland K, Ganeteg U (2009) Uptake of organic nitrogen by plants. New Phytol 182:31–48.

Ono F, Frommer WB, Wirén N (2000) Coordinated diurnal regulation of low- and high-affinity nitrate transporters in tomato. Plant Biol 2:17–23.

Parker C (2009) Observations on the current status of *Orobanche* and *Striga* problems worldwide. Pest Manag Sci 65:453–459.

Peterson CA, Enstone DE, Taylor JH (1999) Pine root structure and its potential significance for root function. Plant Soil 217:203–213.

Pettersson S, Jensen P (1983) Variation among species and varieties in uptake and utilization of potassium. Plant Soil 72:231–237.

Peuke AD, Tischner R (1991) Nitrate uptake and utilisation of aseptically cultivated Spruce seedlings, *Picea abies* (L.) Karst. J Exp Bot 42: 723–728.

Pignone D, Hammer K (2016) Parasitic angiosperms as cultivated plants? Genet Resour Crop Evol 63:1273–1284.

Rennenberg H, Loreto F, Polle A, Brilli F, Fares S, Beniwal R, Gessler A (2006) Physiological responses of forest trees to heat and drought. Plant Biol 8:556–571.

Riaz M, Farooq J, Sakhawat G, Mahmood A, Sadiq M, Yaseen M (2013) Genotypic variability for root/shoot parameters under water stress in some advanced lines of cotton (*Gossypium hirsutum* L.). Gen Mol Res 12:552–561.

Shabala L (2000) Ionic and osmotic components of salt stress specifically modulate net ion fluxes from bean leaf mesophyll. Plant Cell Environ 23:825–837.

Shabala L, Zhang JY, Pottosin I et al. (2016) Cell-type-specific H^+-ATPase activity in root tissues enables K^+ retention and mediates acclimation of Barley (*Hordeum vulgare*) to salinity stress. Plant Physiol 172:2445–2458.

Shi HL, Ma WJ, Song JY, Lu M, Rahman SU, Bui TX, Vu DD, Wang JH, Zhang Y (2017) Physiological and transcriptional responses of *Catalpa Bungeito* drought stress under sufficient- and deficient nitrogen conditions. Tree Physiol 37:1457–1468.

Stromberg JC, Lite SJ, Marler R, Paradzick C, Shafroth PB, Shorrock D, White JM, White MS (2007) Altered stream-flow regimes and invasive plant species: the *Tamarix* case. Glob Ecol Biogeogr 16:381–393.

Sun L, Yu FL, Fang WY, Kronzucker HJ, Shi WM (2016) Biological nitrification inhibition by rice root exudates and its relationship with nitrogen-use efficiency. New Phytol 212:646–656.

Ullah A, Sun H, Yang XY, Zhang XL (2017) Drought coping strategies in cotton: increased crop per drop. Plant Biotechnol J 15:271–284.

Tran TT, Kano-Nakata M, Takeda M, Menge D, Mitsuya S, Inukai Y, Yamauchi A (2014) Nitrogen application enhanced the expression of developmental plasticity of root systems triggered by mild drought stress in rice. Plant Soil 378:139–152.

Tsay YF, Schroeder JI, Feldmann KA, Crawford NM (1993) The herbicide sensitivity gene CHL1 of *Arabidopsis* encodes a nitrate-inducible nitrate transporter. Cell 72:705–713.

Walker HA (2008) Floristics and physiognomy determine migrant landbird response to tamarisk (*Tamarix ramosissima*) invasion in riparian areas. Auk 125:520–531.

Wang L, Macko S (2011) Constrained preferences in nitrogen uptake across plant species and environments. Plant Cell Environ 34:525–534.

Wang YY, Hsu PK, Tsay YF (2012) Uptake, allocation and signaling of nitrate. Trends Plant Sci 17:458–467.

Waraich EA, Ahmad R, Ashraf MY, Ahmad SM (2011) Improving agricultural water use efficiency by nutrient management in crop plants. Acta Agr Scand B-S P 61:291–304.

Warren CR (2009) Does nitrogen concentration affect relative uptake rates of nitrate, ammonium, and glycine? J Plant Nutr Soil Sci 172:224–229.

Warren CR (2014) Organic N molecules in the soil solution: what is known, what is unknown and the path forwards. Plant Soil 375:1–19.

Wilkinson S, Bacon MA, Davies WJ (2007) Nitrate signalling to stomata and growing leaves: interactions with soil drying, ABA, and xylem sap pH in maize. J Exp Bot 58:1705–1716.

Xiao SC, Xiao HL, Si JH, Liu FM (2005) Growth characteristics of *Tamarix ramosissima* in arid regions of China (in Chinese). Acta Bot Boreal-Occident Sin 25:1012–1016.

Xu Y, Sun T, Yin LP (2006) Application of non-invasive microsensing system to simultaneously measure both H^+ and O_2 fluxes around the pollen tube. J Integr Plant Biol 48:823–831.

Yi H, Calvo-Polanco M, MacKinnon MD, Zwiazek JJ (2008) Responses of ectomycorrhizal *Populus tremuloides* and *Betula papyrifera* seedlings to salinity. Environ Exp Bot 62:357–363.

Yi XP, Zhang YL, Yao HS, Zhang XJ, Luo HH, Gou L, Zhang W (2014) Alternative electron sinks are crucial for conferring photoprotection infield-grown cotton under water deficit during flowering and boll setting stages. Funct Plant Biol 41:737–747.

Zhang CX, Meng S, Li YM, Zhao Z (2014) Net NH_4^+ and NO_3^- fluxes, and expression of NH_4^+ and NO_3^- transporter genes in roots of *Populus simonii* after acclimation to moderate salinity. Trees 28: 1813–1821.

Zhang L, Li GJ, Wang M, Di DW, Sun L, Kronzucker HJ, Shi WM (2018) Excess iron stress reduces root tip zone growth through nitric oxide-mediated repression of potassium homeostasis in *Arabidopsis*. New Phytol 219:259–274.

Zhang Q, Zhang XS (2012) Impacts of predictor variables and species models on simulating *Tamarix ramosissima* distribution in Tarim Basin, northwestern China. J Plant Ecol 3:337–345.

Zhang Y, Zhou ZC, Yang Q (2013) Genetic variations in root morphology and phosphorus efficiency of *Pinus massoniana* under heterogeneous and homogeneous low phosphorus conditions. Plant Soil 364:93–104.

Zong YZ, Shangguan ZP (2014) Nitrogen deficiency limited the improvement of photosynthesis in maize by elevated CO_2 under drought. J Integr Agr 13:73–81.